

Brightening of dark excitons in a single CdTe quantum dot containing a single Mn²⁺ ionM. Goryca,^{1,2,*} P. Plochocka,¹ T. Kazimierczuk,² P. Wojnar,³ G. Karczewski,³ J. A. Gaj,² M. Potemski,¹ and P. Kossacki^{1,2}¹*Laboratoire National des Champs Magnétiques Intenses, CNRS-UJF-UPS-INSA, 38042 Grenoble, France*²*Institute of Experimental Physics, University of Warsaw, ul. Hoża 69, 00-681 Warszawa, Poland*³*Institute of Physics, Polish Academy of Sciences, al. Lotników 32/46, 02-688 Warszawa, Poland*

(Received 16 September 2010; published 20 October 2010)

A promising method to investigate dark exciton transitions in quantum dots is presented. The optical recombination of the dark exciton is allowed when the exciton state is coupled with an individual magnetic impurity (manganese ion). It is shown that the efficient radiative recombination is possible when the exchange interaction with the magnetic ion is accompanied by a mixing of the heavy-light hole states related to an in-plane anisotropy of the quantum dot. It is also shown that the dark exciton recombination is an efficient channel of manganese spin orientation.

DOI: [10.1103/PhysRevB.82.165323](https://doi.org/10.1103/PhysRevB.82.165323)

PACS number(s): 78.67.Hc, 73.21.La, 75.75.-c, 78.55.Et

I. INTRODUCTION

Semiconductor quantum dots (QDs) are among the most promising single-photon emitters.^{1–4} They have potential applications in quantum information processing, and quantum telecommunications due to their seamless integration in semiconductor circuits, their robustness and their relatively easy handling. These advantages are particularly clear in comparison to devices based on atoms, ions, or colloidal nanoparticle systems. Crucially, semiconductor QDs provide the possibility to integrate photonic properties with the spin of an individual magnetic impurity.^{5,6} The magnetic spin can be selectively manipulated and used for information storage.^{7–11} However, the use of semiconductor QDs in a realistic working device requires a reliable control of the excitation process as well as an understanding of the emission channels.

An important but nevertheless, little investigated recombination channel is related to the dark exciton states, i.e., states with total angular momentum equal to 2.¹² Random transitions between dark and bright excitonic states lead to exciton decoherence¹³ and a significant modification of the recombination dynamics which can result in the delayed emission of photons.^{14,15} Despite their importance, dark exciton states are difficult to probe. The radiative recombination of dark excitons is forbidden so that they usually cannot be studied directly using spectroscopic techniques. Their properties can be accessed indirectly by a detailed analysis of the dynamics in time-resolved profiles of the bright exciton photoluminescence.^{14–16} The other possibility is to measure the weak optical transitions under conditions in which the dark exciton recombination is partially allowed. This has been achieved either by the use of the in-plane magnetic field which mixes the heavy-light hole states^{17,18} or by placing the QD in a micropillar which enhances the coupling of the exciton with light.¹⁹

Here we present an investigation of dark exciton optical transitions which are allowed due to the simultaneous spin flip of coupled single magnetic impurity. We analyze the dark exciton wave function and show that the radiative recombination of dark excitons is efficient only when the exchange interaction with the magnetic ion is accompanied by

mixing of the heavy-light hole states, related to an in-plane anisotropy of the QD. To demonstrate the interplay of both mechanisms, high magnetic field spectroscopy has been employed. We determine all relevant parameters such as the dark exciton oscillator strength, the in-plane anisotropy, and the exchange interaction. Additionally, we show that the dark exciton recombination is an efficient mechanism of the spin orientation of the magnetic ion.

II. SAMPLE AND EXPERIMENTAL SETUP

The sample, which was grown using molecular beam epitaxy, contains a single layer of self-assembled CdTe QDs with a low concentration of Mn²⁺ ions, embedded in a ZnTe matrix. The Mn²⁺ concentration was adjusted to obtain a significant number of QDs containing exactly one Mn²⁺ ion.²⁰ For the measurements, the sample was placed in a microphotoluminescence (μ -PL) setup comprising of piezoelectric x - y - z stages and a microscope objective. The μ -PL system was kept at the temperature of 4.2 K in a cryostat placed in a resistive magnet producing magnetic field up to 28 T. The field was applied in the Faraday configuration, parallel to the growth axis of the sample. The PL of the QDs was excited either above the gap of the ZnTe barrier (at 532 nm) or using a tunable dye laser in the range 570–610 nm. Both the exciting and the collected light were transmitted through a monomode fiber coupled directly to the microscope objective. The use of the monomode fiber combined with polarization optics outside the cryostat permits the control of the circular polarization of both the exciting and detected light.

III. EXPERIMENTAL RESULTS

The diameter of both the excitation and detection spot was less than 2 μ m, which allows us to select spectra of different single QDs containing a single Mn²⁺ ion. Representative results for two selected QDs with different in-plane anisotropy are shown in the insets of Fig. 1. Characteristic PL spectra contain a neutral exciton (X) lines split into sextuplets due to the X -Mn exchange interaction.^{5,21} The total spin of the Mn²⁺ ion is 5/2, and it has six possible projections

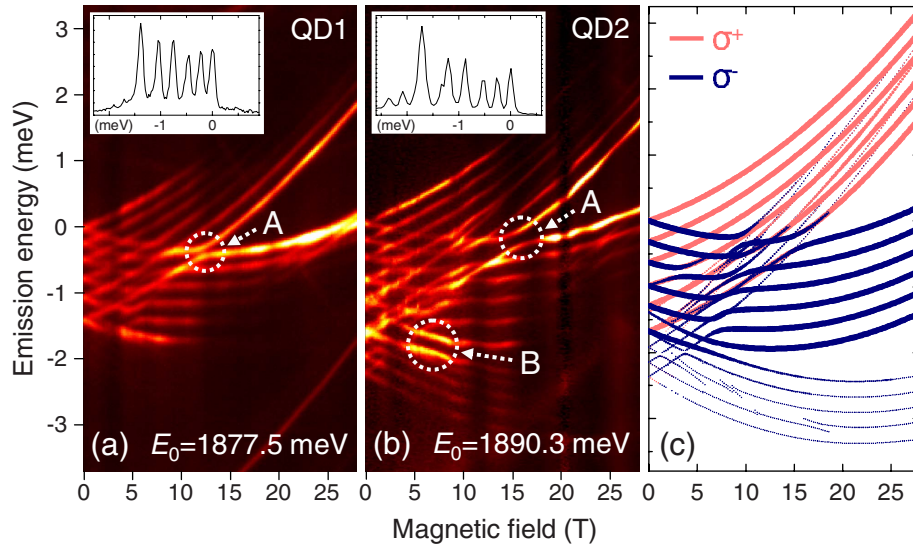


FIG. 1. (Color online) [(a) and (b)] Color-scale plots of the PL spectra of two single Mn-doped QDs as a function of magnetic field. Two dots (QD1 and QD2) differ by in-plane anisotropy. The vertical scale of each panel is shifted by E_0 . Insets: PL spectra at $B=0$. (c) Simulation of the optical transitions in the QD2 with the model described in text. The line thickness corresponds to the oscillator strength of the transitions.

onto the direction of highly anisotropic excitonic spin. Thus, each of the six possible spin states of the ion is related to a specific component of the excitonic sextuplet for a given circular polarization. As in our previous work,¹⁰ we have selected dots which have a nonmagnetic QD as a close neighbor. The resonant excitation of this dot is followed by a spin conserving X transfer to the Mn-doped QD.²² This permits the efficient and selective excitation of the luminescent dot as well as the selection of the spin polarization of excitons injected into the dot. As a result, the control over the Mn^{2+} spin orientation is possible due to the interaction of the magnetic ion with spin-polarized carriers.¹⁰

Figures 1(a) and 1(b) shows the evolution of X PL spectra with magnetic field, measured without polarization resolution for the two selected QDs. To elucidate the most characteristic features of this evolution we initially focus on Fig. 1(a) showing the QD with the smaller in-plane anisotropy. In the magnetic field, the exciton sextuplet splits into two distinct Zeeman branches corresponding to σ^+ and σ^- circular polarizations for the upper and lower branch, respectively. The lowest component of each branch corresponds to the Mn^{2+} spin antiparallel to the exciton spin.⁵ The resonant excitation with σ^- polarization, combined with the magnetic field which significantly slows down the Mn spin relaxation,²³ prevents the Mn^{2+} spin from thermalizing.¹⁰ Therefore all six lines are visible in both branches up to magnetic fields ~ 15 T.

At a magnetic field of around 12 T, an anticrossing of the outermost lines of both branches is clearly visible [“A” in Fig. 1(a)]. These two lines correspond to the same $-5/2$ state of the Mn^{2+} spin but two opposite spin states of X . At this field, the excitonic Zeeman splitting exactly compensates the X -Mn exchange interaction. The splitting (anticrossing) of these two lines is then simply due to the in-plane anisotropy of the QD, acting via the anisotropic component of the electron-hole (e - h) exchange interaction, as observed for ex-

citonic lines in the absence of magnetic field for nonmagnetic QD.²⁴ As we have checked, the two split lines show linear polarization (presumably along the symmetry axes of the anisotropic dot), in contrast to the remaining sextuplet lines which are polarized circularly. The anisotropic exchange splitting, determined from the anticrossing, is equal to $60 \mu\text{eV}$ for QD1 in Fig. 1(a), and $230 \mu\text{eV}$ for QD2 in Fig. 1(b).

Our optical method to align the Mn^{2+} spin against the action of the external magnetic field¹⁰ becomes less efficient at magnetic fields above ~ 15 T. This is due to the accelerated spin-lattice relaxation of the Mn^{2+} spin at high magnetic fields.²⁵ As a result, the Mn^{2+} spin orientation thermalizes and the excitonic lines related to the less populated spin states vanish.

Strikingly, the QD with the larger anisotropic exchange splitting value [Fig. 1(b)] has an additional, albeit weaker, lower branch consisting of only five lines. To understand the origin of this branch one should notice that optical transitions are possible in two situations: (a) the projection of total angular momentum of the exciton on the quantization axis is equal to ± 1 (bright exciton). In this case the transition is dipole allowed and the Mn^{2+} spin projection is conserved during the X recombination. Branches with six lines are related to this kind of recombination. (b) The projection of total angular momentum of the exciton is equal to ± 2 (dark exciton, X_d). Then, in the first approximation the optical transition is dipole forbidden. However, the valence band mixing and the exchange interaction with the Mn^{2+} ion result in a mixing of the electron and hole spin states. As a result, the X_d states have an admixture of the X states with the Mn^{2+} spin projection different by 1. Thus, the X_d recombination is possible when accompanied by the simultaneous spin flip of the Mn^{2+} ion. As there are only five possible transitions between the 6 Mn^{2+} spin states, the PL lines related to X_d present a fivefold splitting. The upper energy branch of X_d is not clearly

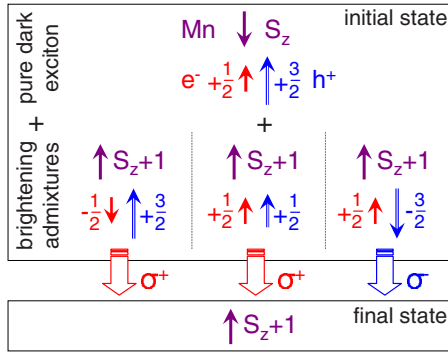


FIG. 2. (Color online) Schematic diagram of X admixtures in the X_d states and possible channels of optical transitions related to the X_d recombination.

visible in our experiment because it overlaps with much stronger X transitions.

IV. DARK EXCITON WAVE FUNCTION

The quantum states of the exciton and Mn^{2+} spin can be described in the basis given by three quantum numbers: $|S_z, \sigma_z, j_z\rangle$ indicating the Mn^{2+} , electron and hole angular momentum projections onto the quantization axis parallel to the magnetic field. Using the available information for the g factors of the carriers and the Mn^{2+} ion,²⁶ we attribute the X_d low-energy branch to the recombination of $|S_z, +1/2, +3/2\rangle$ states. Therefore, to satisfy the selection rules for X_d dipolar recombination the projection of the Mn^{2+} spin must be increased by 1. This implies that each possible X_d recombination is related to a spin flip of the Mn^{2+} ion toward the state polarized opposite to the thermalized state. There are three different admixtures of the X_d states which make this process possible (see Fig. 2). The first one is the state with the opposite spin projection of the electron ($|S_z+1, -1/2, +3/2\rangle$). It is mixed with the X_d state due to the e -Mn exchange interaction. The second admixture, caused by the h -Mn exchange interaction, consists of a light hole with a spin projection different by 1 from the heavy hole of the X_d ($|S_z+1, +1/2, +1/2\rangle$). The last admixed state, $|S_z+1, +1/2, -3/2\rangle$, consists of a heavy hole with a spin projection different by 3 from the spin projection of the original state. This admixture is induced by two interactions acting together: the heavy-light hole mixing, which mixes hole states with spin projection different by 2, and by the h -Mn exchange interaction. A direct experimental evidence for the presence of valence band mixing is provided by the anticrossing of the highest energy line of X_d and the lowest energy line of X at a magnetic field ~ 7 T [labeled “B” in Fig. 1(b)]. These lines correspond to $|+1.5, +1/2, +3/2\rangle$ and $|+2.5, +1/2, -3/2\rangle$ states, respectively.

The radiative recombination related to the first two of these admixtures results in the emission of a photon with σ^+ polarization. The amplitudes of these admixtures depend only on the e -Mn and h -Mn exchange constants, i.e., on the overlap of the Mn^{2+} ion and the carrier wave functions. In contrast, the recombination related to the third admixture produces a σ^- polarized photon. The amplitude of this ad-

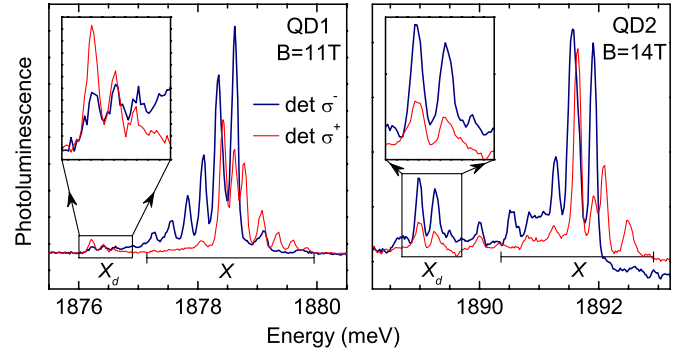


FIG. 3. (Color online) Spectra of the two QDs shown in Fig. 1 taken under excitation with σ^- polarized light with polarization resolved (σ^+ or σ^-) detection for magnetic fields near the anticrossing of lines corresponding to $| -2.5, -1/2, +3/2\rangle$ and $| -2.5, +1/2, -3/2\rangle$ states [A in Figs. 1(a) and 1(b)].

mixture depends not only on the X -Mn exchange interaction but also on the valence band mixing, which, similarly to the anisotropic exchange splitting, results from the in-plane anisotropy of the QD.^{18,27–29} The role of this anisotropy in determining the polarization of the X_d lines is clearly visible in our experiment. Figure 3 shows spectra of the two QDs shown in Fig. 1 for similar excitation conditions and magnetic field near the anticrossing of the lines related to $| -2.5, -1/2, +3/2\rangle$ and $| -2.5, +1/2, -3/2\rangle$ states [A in Figs. 1(a) and 1(b)]. In the X_d region the σ^- polarized lines are much more pronounced with respect to the σ^+ polarized ones for a highly anisotropic QD2.

As a quantitative measure of the X_d oscillator strength for both circular polarizations we use the X_d/X intensity ratio. Since this ratio depends on the excitation power,³⁰ one should use identical excitation conditions to be able to compare its value for different QDs. Experimentally, this is achieved by choosing the same XX/X intensity ratio equal in our case to 1/3. The XX intensity increases roughly quadratically with the excitation power while the X intensity follows linear power dependence.^{31,32} Thus, this ratio gives a measure of the excitation efficiency.

A strong increase in the X_d/X intensity ratio in σ^+ polarization with increasing X -Mn exchange constant (calculated from the splitting of excitonic sextuplet) is clearly visible in Fig. 4(a). It confirms the origin of the first two recombination channels described above. However, the X_d oscillator strength for σ^- polarization depends both on the X -Mn exchange interaction and the QD anisotropy. To elucidate the role of the anisotropy, we can use the circular polarization of the X_d . Figure 4(b) shows that it evolves toward σ^- as the anisotropic exchange splitting increases. Therefore, we conclude that a high in-plane anisotropy of the QD leads to a strong mixing of light and heavy holes, which combined with the presence of the Mn^{2+} ion is the reason for the strong σ^- polarization and high intensity of the X_d spectrum. It is important to note that for nonmagnetic QDs showing similar anisotropy¹⁸ the optical transitions of X_d are not observed, except in the presence of a strong in-plane magnetic field.

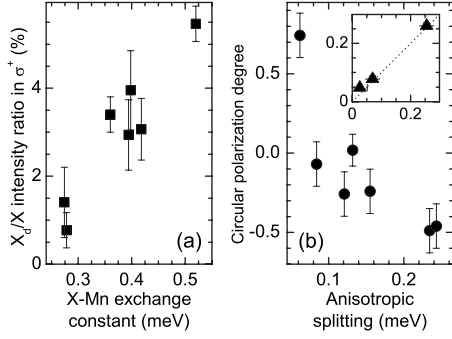


FIG. 4. (a) X_d/X intensity ratio in σ^+ polarization vs X-Mn exchange constant. (b) Degree of circular polarization of X_d spectrum vs anisotropic exchange splitting of the QD. A value of -1 denotes pure σ^- polarization while a value of $+1$ refers to pure σ^+ polarization. Inset: the width of splitting between the $|+1.5, +1/2, +3/2\rangle$ and $|-2.5, +1/2, -3/2\rangle$ lines [B in Fig. 1(b)] calculated from the model vs splitting between these lines determined directly from the PL for those QDs for which it was possible.

V. MN SPIN ORIENTATION MEDIATED BY DARK EXCITONS

As previously shown,¹⁰ multiple events of injection and recombination of σ^- polarized excitons in a single Mn-doped QD induce the spin polarization of the Mn^{2+} ion toward the states with positive spin projection. Since under σ^- polarized excitation the lower energy X_d branch is always visible for anisotropic QDs and each recombination of such X_d involves an increase in the Mn^{2+} spin projection by 1, these recombinations can play the role of an effective Mn^{2+} spin orientation mechanism. In our experiment the X_d/X intensity ratio for a highly anisotropic QD was as high as 10%. This is comparable to the probability of a spin flip of the Mn^{2+} ion per one recombination of the X which was estimated to be $\sim 10\%$ in Ref. 10. While this orientation mechanism should be present for both circular polarizations of excitation, only the case of σ^- is fully seen. Under σ^+ polarized excitation, which decreases the Mn^{2+} spin projection,¹⁰ the high-energy branch of X_d should be populated and the low-energy branch should be virtually invisible. The latter is, indeed, confirmed in our experiment. However, it is not possible to observe directly the high energy X_d branch since it occurs in the same energy region as the much stronger X lines.

VI. MODEL

A quantitative description of key features of the data in Figs. 1(a) and 1(b) is provided by a simple model with the initial state of the QD after excitation event given by the following Hamiltonian,^{17,18,33–36}

$$\mathcal{H} = g_{Mn}\mu_B\vec{B} \cdot \vec{S} + g_e\mu_B\vec{B} \cdot \vec{\sigma} + g_h\mu_B\vec{B} \cdot \vec{j} - I_e\vec{S} \cdot \vec{\sigma} - I_h\vec{S} \cdot \vec{j} + \sum_{i=x,y,z} (a_{ij}\sigma_i + b_{ij}j_i^3\sigma_i) - \gamma_j^2 + \beta(j_x^2 - j_y^2),$$

where S , σ , and j are the Mn^{2+} , electron and hole spin op-

erators, respectively, the first three terms represent the Zeeman energy of the Mn^{2+} ion, the electron and the hole, I_e and I_h are the e -Mn and h -Mn exchange interaction constants, a_i and b_i are e - h spin-spin coupling constants, 2γ is the heavy-light hole splitting and β represents the strength of the heavy-light hole mixing. The first term is also the Hamiltonian of the final state of the system after the exciton recombination. We also introduced an additional, phenomenological term related to the excitonic diamagnetic shift to facilitate a comparison of the model and experimental data.

The energies of the optical transitions versus magnetic field, calculated using this Hamiltonian for the two circular polarizations, are plotted in Fig. 1(c). The calculations clearly reproduce the key features of the experimental data in Figs. 1(a) and 1(b), such as, for example, the X-Mn exchange splitting and the anisotropic exchange splitting. All parameters in the Hamiltonian [except for γ assumed to be 15 meV (Ref. 29)] can be extracted by fitting to the experimental data. In particular, the heavy-light hole mixing can be estimated using the degree of circular polarization of X_d lines. Such an approach permits an estimation of the β parameter even for those QDs, for which the anticrossing between the $|+1.5, +1/2, +3/2\rangle$ and $|-2.5, +1/2, -3/2\rangle$ lines [B in Fig. 1(b)] is not clearly visible. As shown in the inset of Fig. 4(b) the obtained value of this anticrossing remains in very good agreement with the value estimated directly from PL data. This confirms the proposed mechanism of X_d brightening.

VII. CONCLUSIONS

We have used a QD with a single magnetic impurity (Mn^{2+}) to investigate the dark exciton transitions. The X-Mn exchange interaction, when combined with a mixing of the heavy-light hole states induced by the QD in-plane anisotropy, allows X_d recombination accompanied by a simultaneous Mn^{2+} spin flip. Thus the X_d recombination can act as an effective Mn^{2+} spin orientation mechanism for highly anisotropic QDs. High magnetic fields have been used to spectrally separate the PL lines related to X and X_d transitions and to extract the important QD parameters (e.g., the anisotropic exchange splitting). The simple Hamiltonian, which describes this system, reproduces correctly all the key features of the PL spectra of the QD in high magnetic field.

ACKNOWLEDGMENTS

This work was supported by the Polish Ministry of Science and Higher Education as research grants in years 2006–2011, by the EuromagNetII, by the sixth Research Framework Programme of EU (Contract No. MTKD-CT-2005-029671), by the CNRS PICS-4340 Programme, by NCBIr project *Lider* and by the Foundation for Polish Science. Two of us (P.P. and P.K.) are financially supported by the EU under FP7, Contracts No. 221249 “SESAM” and No. 221515 “MOCNA,” respectively. We thank Anna Trojnar and Marek Korkusiński for fruitful discussions.

*mateusz.goryca@fuw.edu.pl

- ¹P. Michler, A. Kiraz, C. Becher, W. V. Schoenfeld, P. M. Petroff, L. Zhang, E. Hu, and A. Imamoğlu, *Science* **290**, 2282 (2000).
- ²P. Michler, A. Imamoğlu, M. D. Mason, P. J. Carson, G. F. Strouse, and S. K. Buratto, *Nature (London)* **406**, 968 (2000).
- ³C. Santori, M. Pelton, G. Solomon, Y. Dale, and Y. Yamamoto, *Phys. Rev. Lett.* **86**, 1502 (2001).
- ⁴V. Zwiller, H. Blom, P. Jonsson, N. Panev, S. Jeppesen, T. Tsegaye, E. Goobar, M.-E. Pistol, L. Samuelson, and G. Björk, *Appl. Phys. Lett.* **78**, 2476 (2001).
- ⁵L. Besombes, Y. Léger, L. Maingault, D. Ferrand, H. Mariette, and J. Cibert, *Phys. Rev. Lett.* **93**, 207403 (2004).
- ⁶A. Kudelski, A. Lemaître, A. Miard, P. Voisin, T. C. M. Graham, R. J. Warburton, and O. Krebs, *Phys. Rev. Lett.* **99**, 247209 (2007).
- ⁷C. Le Gall, L. Besombes, H. Boukari, R. Kolodka, J. Cibert, and H. Mariette, *Phys. Rev. Lett.* **102**, 127402 (2009).
- ⁸D. E. Reiter, T. Kuhn, V. M. Axt, and P. Machnikowski, *J. Phys.: Conf. Ser.* **193**, 012101 (2009).
- ⁹D. E. Reiter, T. Kuhn, and V. M. Axt, *Phys. Rev. Lett.* **102**, 177403 (2009).
- ¹⁰M. Goryca, T. Kazimierzczuk, M. Nawrocki, A. Golnik, J. A. Gaj, P. Kossacki, P. Wojnar, and G. Karczewski, *Phys. Rev. Lett.* **103**, 087401 (2009).
- ¹¹Ł. Cywiński, *Phys. Rev. B* **82**, 075321 (2010).
- ¹²J. D. Cuthbert and D. G. Thomas, *Phys. Rev.* **154**, 763 (1967).
- ¹³P. Palinginis, H. Wang, S. V. Goupalov, D. S. Citrin, M. Dobrowolska, and J. K. Furdyna, *Phys. Rev. B* **70**, 073302 (2004).
- ¹⁴S. A. Crooker, T. Barrick, J. A. Hollingsworth, and V. I. Klimov, *Appl. Phys. Lett.* **82**, 2793 (2003).
- ¹⁵O. Labeau, P. Tamarat, and B. Lounis, *Phys. Rev. Lett.* **90**, 257404 (2003).
- ¹⁶G. Bacher, R. Weigand, J. Seufert, V. D. Kulakovskii, N. A. Gippius, A. Forchel, K. Leonardi, and D. Hommel, *Phys. Rev. Lett.* **83**, 4417 (1999).
- ¹⁷M. Bayer, G. Ortner, O. Stern, A. Kuther, A. A. Gorbunov, A. Forchel, P. Hawrylak, S. Fafard, K. Hinzer, T. L. Reinecke, S. N. Walck, J. P. Reithmaier, F. Klopff, and F. Schäfer, *Phys. Rev. B* **65**, 195315 (2002).
- ¹⁸K. Kowalik, O. Krebs, A. Golnik, J. Suffczyński, P. Wojnar, J. Kossut, J. A. Gaj, and P. Voisin, *Phys. Rev. B* **75**, 195340 (2007).
- ¹⁹M. Winger, A. Badolato, K. J. Hennessy, E. L. Hu, and A. Imamoğlu, *Phys. Rev. Lett.* **101**, 226808 (2008).
- ²⁰P. Wojnar, J. Suffczyński, K. Kowalik, A. Golnik, G. Karczewski, and J. Kossut, *Phys. Rev. B* **75**, 155301 (2007).
- ²¹J. Fernández-Rossier, *Phys. Rev. B* **73**, 045301 (2006).
- ²²T. Kazimierzczuk, J. Suffczyński, A. Golnik, J. A. Gaj, P. Kossacki, and P. Wojnar, *Phys. Rev. B* **79**, 153301 (2009).
- ²³M. Goryca, D. Ferrand, P. Kossacki, M. Nawrocki, W. Pacuski, W. Maślana, J. A. Gaj, S. Tatarenko, J. Cibert, T. Wojtowicz, and G. Karczewski, *Phys. Rev. Lett.* **102**, 046408 (2009).
- ²⁴D. Gammon, E. S. Snow, B. V. Shanabrook, D. S. Katzer, and D. Park, *Science* **273**, 87 (1996).
- ²⁵T. Strutz, A. M. Witowski, and P. Wyder, *Phys. Rev. Lett.* **68**, 3912 (1992).
- ²⁶L. Besombes, L. Marsal, K. Kheng, T. Charvolin, L. S. Dang, A. Wasiela, and H. Mariette, *J. Cryst. Growth* **214-215**, 742 (2000).
- ²⁷M. Bayer, A. Kuther, A. Forchel, A. Gorbunov, V. B. Timofeev, F. Schäfer, J. P. Reithmaier, T. L. Reinecke, and S. N. Walck, *Phys. Rev. Lett.* **82**, 1748 (1999).
- ²⁸A. V. Koudinov, I. A. Akimov, Y. G. Kusrayev, and F. Henneberger, *Phys. Rev. B* **70**, 241305 (2004).
- ²⁹Y. Léger, L. Besombes, L. Maingault, and H. Mariette, *Phys. Rev. B* **76**, 045331 (2007).
- ³⁰L. Besombes, Y. Leger, L. Maingault, D. Ferrand, H. Mariette, and J. Cibert, *Phys. Rev. B* **71**, 161307 (2005).
- ³¹K. Brunner, G. Abstreiter, G. Böhm, G. Tränkle, and G. Weimann, *Phys. Rev. Lett.* **73**, 1138 (1994).
- ³²J. Suffczyński, T. Kazimierzczuk, M. Goryca, B. Piechal, A. Trajnerowicz, K. Kowalik, P. Kossacki, A. Golnik, K. P. Korona, M. Nawrocki, J. A. Gaj, and G. Karczewski, *Phys. Rev. B* **74**, 085319 (2006).
- ³³H. W. van Kesteren, E. C. Cosman, W. A. J. A. van der Poel, and C. T. Foxon, *Phys. Rev. B* **41**, 5283 (1990).
- ³⁴E. L. Ivchenko, A. Y. Kaminski, and U. Rössler, *Phys. Rev. B* **54**, 5852 (1996).
- ³⁵A. A. Toropov, E. L. Ivchenko, O. Krebs, S. Cortez, P. Voisin, and J. L. Gentner, *Phys. Rev. B* **63**, 035302 (2000).
- ³⁶S. J. Cheng and P. Hawrylak, *EPL* **81**, 37005 (2008).